

See discussions, stats, and author profiles for this publication at: <https://www.researchgate.net/publication/12501906>

# Taylor, J.R., Fang, M.M., & Nie, S.M. Probing specific sequences on single DNA molecules with bioconjugated fluorescent nanoparticles. Anal. Chem. 72, 1979–1986

ARTICLE in ANALYTICAL CHEMISTRY · JUNE 2000

Impact Factor: 5.64 · DOI: 10.1021/ac9913311 · Source: PubMed

---

CITATIONS

227

---

READS

30

3 AUTHORS, INCLUDING:



Mic Fang

University of Iowa

2 PUBLICATIONS 252 CITATIONS

SEE PROFILE



Shuming Nie

Emory University

212 PUBLICATIONS 35,333 CITATIONS

SEE PROFILE

# Probing Specific Sequences on Single DNA Molecules with Bioconjugated Fluorescent Nanoparticles

Jason R. Taylor, Michelle M. Fang, and Shuming Nie\*

Department of Chemistry, Indiana University, Bloomington, Indiana 47405

**Nanometer-sized fluorescent particles (latex nanobeads) have been covalently linked to DNA binding proteins to probe specific sequences on stretched single DNA molecules. In comparison with single organic fluorophores, these nanoparticle probes are brighter, are more stable against photobleaching, and do not suffer from intermittent on/off light emission (blinking). Specifically, we demonstrate that the site-specific restriction enzyme EcoRI can be conjugated to 20-nm fluorescent nanoparticles and that the resulting nanoconjugates display DNA binding and cleavage activities of the native enzyme. In the absence of cofactor magnesium ions, the EcoRI conjugates bind to specific sequences on double-stranded DNA but do not initiate enzymatic cutting. For single DNA molecules that are stretched and immobilized on a solid surface, nanoparticles bound at specific sites can be directly visualized by multicolor fluorescence microscopy. Direct observation of site-specific probes on single DNA molecules opens new possibilities in optical gene mapping and in the fundamental study of DNA–protein interactions.**

Recent advances in ultrasensitive instrumentation have allowed the detection, identification, and dynamic studies of single molecules and single nanoparticles at room temperature.<sup>1</sup> These studies represent the ultimate sensitivity and yield new information that is not available from population-averaged measurements. In particular, single-molecule imaging and manipulation can provide new insights into the dynamics and function of biomacromolecules such as nucleic acids and proteins. Recent advances have examined the mechanical properties of single DNA molecules,<sup>2–4</sup>

the catalytic rates of single enzymes,<sup>5,6</sup> the mechanism of force generation in single molecular motors,<sup>7–10</sup> and the interactions between single enzymes and DNA molecules.<sup>11–14</sup> Current single-molecule studies, however, are based mainly on the use of organic fluorophores that often suffer from photobleaching, low signal intensities, and random on/off light emission (blinking). Photobleaching is usually caused by sudden decomposition of the emitter; it is the main factor limiting the maximum number of photons that is obtainable from a fluorophore. Low signal intensities reduce the accuracy with which the spatial position of a single molecule can be determined. Intermittent light emission causes problems in real-time studies of biomolecular dynamics such as protein folding, signal transduction, and enzymatic catalysis.

We report a class of nanometer-sized luminescent particles that are covalently linked to DNA binding proteins which allow for the study of specific sequences on single DNA molecules. Three

\* Corresponding author. Tel: 812-855-6620. Fax: 812-855-8300. Email: nie@indiana.edu

- (1) For reviews, see (a) Moerner, W. E.; Orrit, M. *Science (Washington, D.C.)* **1999**, *283*, 1670–1676. (b) Xie, X. S.; Trautman, J. K. *Annu. Rev. Phys. Chem.* **1998**, *59*, 441–480. (c) Nie, S.; Zare, R. N. *Annu. Rev. Biophys. Biomol. Struct.* **1997**, *26*, 567–596. (d) Keller, R. A.; Ambrose, W. P.; Goodwin, P. M.; Jett, J. H.; Martin, J. C.; Wu, M. *Appl. Spectrosc.* **1996**, *50*, 12A–32A.
- (2) (a) Perkins, T.; Smith, D. E.; Chu, S. *Science (Washington, D.C.)* **1994**, *264*, 819–822. (b) Perkins, T.; Quake, S. R.; Smith, D. E.; Chu, S. *Science (Washington, D.C.)* **1994**, *264*, 822–826. (c) Perkins, T. T.; Smith, D. E.; Chu, S. *Science (Washington, D.C.)* **1997**, *276*, 2016–2021.
- (3) (a) Smith, S. B.; Cui, Y.; Bustamante, C. *Science (Washington, D.C.)* **1996**, *271*, 795–799. (b) Baumann, C. G.; Smith, S. B.; Bloomfield, V. A.; Bustamante, C. *Proc. Natl. Acad. Sci. U.S.A.* **1997**, *94*, 6185–6190.

- (4) (a) Strick, T. R.; Allemand, J.-F.; Bensimon, D.; Bensimon, A.; Croquette, A. *Science (Washington, D.C.)* **1996**, *271*, 1835–1837. (b) Cluzel, P.; Lebrun, A.; Heller, C.; Lavery, R.; Viovy, J.-L.; Chatenay, D.; Caron, F. *Science (Washington, D.C.)* **1996**, *271*, 792–794.
- (5) (a) Xue, Q.; Yeung, E. S. *Nature (London)* **1995**, *373*, 681–682. (b) Craig, D. B.; Arriaga, E.; Wong, J. C. Y.; Lu, H.; Dovichi, N. J. *J. Am. Chem. Soc.* **1996**, *118*, 5245–5253.
- (6) Lu, H. P.; Xun, L.; Xie, X. S. *Science (Washington, D.C.)* **1998**, *282*, 1877–1882.
- (7) Mehta, A. D.; Rief, M.; Spudich, J. A.; Smith, D. A.; Simmons, R. M. *Science (Washington, D.C.)* **1999**, *283*, 1689–1695.
- (8) (a) Funatsu, T.; Harada, Y.; Tokunaga, M.; Saito, K.; Yanagida, T. *Nature (London)* **1995**, *374*, 555–559. (b) Vale, R. D.; Funatsu, T.; Pierce, D. W.; Romberg, L.; Harada, Y.; Yanagida, T. *Nature (London)* **1996**, *380*, 451–453. (c) Ishijima, A.; Kojima, H.; Funatsu, T.; Tokunaga, M.; Higuchi, H.; Tanaka, H.; Yanagida, T. *Cell* **1998**, *92*, 161–171. (d) Kitamura, K.; Tokunaga, M.; Iwane, A. H.; Yanagida, T. *Nature (London)* **1999**, *397*, 129–134.
- (9) (a) Svoboda, K.; Schmidt, C. F.; Schnapp, B. J.; Block, S. M. *Nature (London)* **1993**, *365*, 721–727. (b) Svoboda, K.; Block, S. M. *Cell* **1994**, *77*, 773–784. (c) Visscher, K.; Schnitzer, M. J.; Block, S. M. *Nature (London)* **1999**, *400*, 184–189.
- (10) (a) Noji, H.; Yasuda, R.; Yoshida, M.; Kinoshita, K., Jr. *Nature (London)* **1997**, *386*, 299. (b) Kinoshita, K., Jr.; Yasuda, R.; Noji, H.; Ishiwata, S.; Yoshida, M. *Cell* **1998**, *93*, 21.
- (11) (a) Yin, H.; Wang, M. D.; Svoboda, K.; Landick, R.; Block, S. M.; Gelles, J. *Science (Washington, D.C.)* **1995**, *270*, 1653–1657. (b) Wang, M. D.; Schnitzer, M. J.; Yin, H.; Landick, R.; Gelles, J.; Block, S. M. *Science (Washington, D.C.)* **1998**, *282*, 902–907.
- (12) (a) Kellermayer, M. S. Z.; Smith, S. B.; Granzier, H. L.; Bustamante, C. *Science (Washington, D.C.)* **1997**, *276*, 1112. (b) Bustamante, C.; Guthold, M.; Zhu, X. S.; Yang, G. L. *J. Biol. Chem.* **1999**, *274*, 16665–16668.
- (13) Harada, Y.; Funatsu, T.; Murakami, K.; Nonoyama, Y.; Ishihama, A.; Yanagida, T. *Biophys. J.* **1999**, *76*, 709–715.
- (14) Shivashankar, G. V.; Feingold, M.; Krichevsky, O.; Libchaber, A. *Proc. Natl. Acad. Sci. U.S.A.* **1999**, *96*, 7916–7921.

types of nanoparticles are potentially useful as single-molecule labels, in particular, latex fluorescent nanospheres (commercially available), luminescent quantum dots (recently developed by Alivisatos's group and our own group),<sup>15,16</sup> and optically active metal nanoparticles.<sup>17</sup> In this paper, we focus specifically on 20-nm fluorescent latex particles that are conjugated to proteins through amide bond formation. Unlike single dye molecules, each nanoparticle contains about 100–200 molecules of an embedded dye that is protected from the outside environment. As such, these fluorescent nanoparticles are highly resistant to photobleaching and emit bright and steady (no blinking) fluorescence.

Our results show that fluorescent nanoparticles conjugated with the restriction enzyme EcoRI can recognize and cleave lambda bacteriophage DNA ( $\lambda$ -DNA). If a chelating agent such as EDTA is used to remove the cofactor magnesium ion ( $Mg^{2+}$ ), the bioconjugated nanoparticles bind to specific sequences on stretched DNA but do not initiate enzymatic cutting. Thus, single-particle detection methods can be used to directly visualize specific sequences on large genomic DNA. Single DNA molecules are detected by the green fluorescence (530 nm) of an intercalation dye, while the bound nanoparticles are observed because of their yellow-orange fluorescence (580–620 nm).

## MATERIALS AND METHODS

The general experiment design involves: (i) conjugating carboxylate-modified fluorescent nanoparticles to DNA binding proteins; (ii) incubating the nanoparticles and DNA in solution at 37 °C for efficient binding; (iii) staining the DNA with a fluorescent intercalation dye; (iv) stretching the stained DNA into linear forms, and immobilizing the stretched DNA on a glass surface; and (v) imaging the stretched DNA and the bound nanoparticles by multicolor fluorescence microscopy. In the following, we describe each of these steps in detail.

**Bioconjugation.** Nanoparticle bioconjugation was achieved by using the cross-linking reagent 1-ethyl-3-(3-dimethyl-aminopropyl) carbodiimide (EDAC). This compound reacts with the surface carboxylate ( $-COOH$ ) group on the nanoparticle to yield an *O*-acyl-isourea active intermediate.<sup>18</sup> This intermediate is then attacked by a primary amine ( $-NH_2$ ) group of the protein's lysine side chain, forming a stable covalent bond between the protein and the particle. One drawback to this procedure is that the intermediate formed in the EDAC reaction is subject to hydrolysis in aqueous media.<sup>19</sup> To increase the reaction yield, we added a second reagent *N*-hydroxysulfosuccinimide (sulfo-NHS) to form a more stable active ester intermediate. This intermediate is less susceptible to hydrolysis, while at the same time reacts more rapidly with amines.<sup>20</sup> Thus, 1 mg of protein (histone, bovine serum albumin, or EcoRI) was added to 100  $\mu$ L of MES buffer

(pH 6.0) containing 20-nm carboxylate-modified fluorescent nanoparticles (2 wt %) ( $\lambda_{ex}/\lambda_{em}$  = 560 nm/620 nm, Molecular Probes, Eugene, OR). After 15 minutes, 0.4 mg of EDAC and 1.0 mg of sulfo-NHS were added, and the mixture was vortexed slowly for 2 h. Excess protein (not conjugated to particles) was removed by filtration through a G-75 microspin column (Pharmacia Biotech, Piscataway, NJ) or by dialysis separation with a 50 000 MW Spectra/Por dialyzer (Spectrum, Santa Clara, CA).

On the basis of the relative UV-vis absorption signals of the proteins and the particles, the number of protein molecules per particle was estimated to be about 5–10. At this level of conjugation, most of the attached protein appeared to be biologically active because the nanoconjugates showed efficient DNA cutting abilities (as compared with the free enzyme at similar concentrations). However, we could not rule out that a small portion of the attached enzyme molecules was deactivated by chemical cross-linking.

**DNA Stretching and Immobilization.**  $\lambda$ -DNA concatemers were prepared by incubating 100 ng  $\lambda$ -DNA (monomer) with five units of T4 DNA ligase in 50-mM Tris buffer containing 10-mM  $MgCl_2$ , 1-mM ATP, and 20-mM BSA overnight at 15 °C. For DNA stretching and immobilization, glass cover slips (24 mm  $\times$  50 mm, Fisher Scientific, Pittsburgh, PA) were cleaned in a 70% concentrated  $H_2SO_4$ /30%  $H_2O_2$  solution for 30 min, rinsed in ultrapure water, and wiped clean with spectrophotometric-grade methanol. Polylysine-coated coverslips were prepared by spreading 10  $\mu$ L of a 5.5  $\mu$ g/mL polylysine solution between two coverslips and allowing spontaneous adsorption to occur. After incubating for 1 h, the coverslips were separated and dried in air for 30 min.  $\lambda$ -DNA (38 kb) and coliphage T4 DNA (167 kb) were counterstained with a fluorescent intercalating dye (YOYO-1, Molecular Probes, Eugene, OR). The DNA was labeled at a ratio of four base pairs per dye molecule (bp/dye = 4) by mixing an aliquot of DNA sample with a specific volume of freshly prepared  $10^{-7}$  M dye solution (10-mM Tris buffer, pH 7.6, and 1% 2-mercaptoethanol). The DNA/YOYO-1 solution was incubated for approximately 30 min in a dark room and was then diluted to  $10^{-10}$  M in a 35 mM Tris/3.5 mM EDTA buffer (pH 7.6). The labeled DNA molecules were stretched and immobilized on polylysine-coated coverslips by a laminar-flow method.<sup>21</sup> Briefly, a 7- $\mu$ L aliquot of the  $10^{-10}$  M labeled DNA solution was placed on one end of a coated coverslip, while a clean coverslip was clamped on top to initiate laminar flow. After about 10–15 min, the DNA molecules were simultaneously stretched and immobilized on the polylysine surface.

**Multicolor Fluorescence Imaging.**  $\lambda$ -DNA concatemers,  $\lambda$ -DNA monomers, and T4 DNA were incubated with the bioconjugate nanoparticles (e.g., histone, BSA, EcoRI) in a 35 mM Tris buffer containing 3.5 mM EDTA and 0.5 mg/mL BSA for 30–60 min at 37 °C. The molar ratios of the nanoparticles to DNA were about 5:1. This particle-to-DNA ratio yielded excellent results because the particle binding efficiency was high and the background interference (caused by unbound particles) was fairly low. The DNA molecules with bound bioconjugate nanoparticles were stretched and immobilized on polylysine-coated coverslips, as described above. Multicolor fluorescence imaging was accomplished by using a Nikon inverted microscope, a 100 W mercury arc lamp, and a computer-controlled filter wheel (Sutter Instru-

(15) Bruchez, M. J., Jr.; Moronne, M. M.; Gin, P.; Weiss, S.; Alivisatos, P. A. *Science (Washington, D.C.)* **1998**, *281*, 2013–2016.

(16) Chan, W. C. W.; Nie, S. *Science (Washington, D.C.)* **1998**, *281*, 2016–2018.

(17) (a) Nie, S.; Emory, S. R. *Science (Washington, D.C.)* **1997**, *275*, 1102–1106. (b) Emory, S. R.; Haskins, W. E.; Nie, S. *J. Am. Chem. Soc.* **1998**, *120*, 8009–8010.

(18) Hermanson, G. T. *Bioconjugate Techniques*; Academic Press: New York, 1996.

(19) Gilles, M. A.; Hudson, A. Q.; Borders, C. L. *Anal. Biochem.* **1990**, *184*, 244–248.

(20) Staros, J. V.; Wright, R. W.; Swingle, D. M. *Anal. Biochem.* **1986**, *156*, 220–222.

(21) Lyon, W. A.; Fang, M. M.; Haskins, W. E.; Nie, S. *Anal. Chem.* **1998**, *70*, 1743–1748.

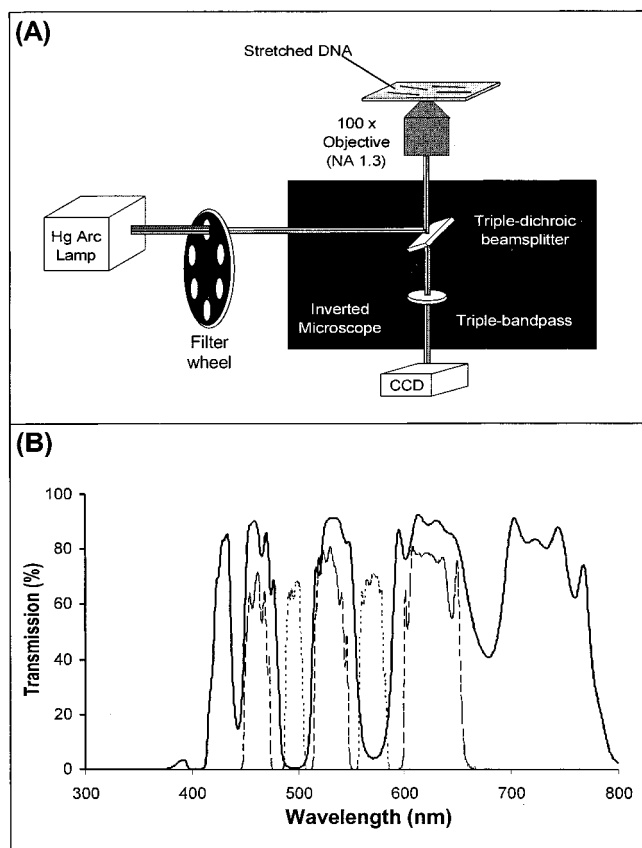


Figure 1. (A) Schematic diagram of the instrumental setup. (B) Transmission curves of the triple-color filter set used in this study. Dotted lines: excitation filters. Dashed lines: triple-band-pass filter. Solid lines: triple-dichroic beam splitter.

ments, Novato, CA) (Figure 1A). The excitation light beam was directed to the sample with an oil immersion objective (100 $\times$ , NA = 1.3) in the epi-illumination configuration. The Stokes shifted fluorescent light was collected through the same objective and passed through a triple-band-pass interference filter (Chroma Tech, Brattleboro, VT). When combined with a triple-dichroic beam splitter, this triple-band-pass filter allowed simultaneous imaging at three emission wavelengths (470, 530, and 620 nm) (Figure 1B). Multicolor fluorescence images (pseudocolor) were acquired by using a thermoelectrically cooled CCD camera (Photometrix, Tucson, AZ) and digital imaging software (Metamorph, Universal Imaging Corp, West Chester, PA). True color images were obtained with a 35-mm Nikon camera attached to the microscope front port.

**Reagents.** All chemicals and biochemicals used in this work were obtained from commercial sources. Poly-L-lysine hydrobromide (MW = 350 000), Trizma base (tris(hydroxymethyl)amino-methane), Trizma hydrochloride (tris(hydroxymethyl)amino-methane hydrochloride), 2-mercaptoethanol, 1-ethyl-3-(3-dimethylaminopropyl)-carbodiimide (EDAC), coliphage T4 DNA,  $\lambda$ -DNA, T4 DNA ligase, histone protein, and bovine serum albumin were purchased from Sigma Chemical Co. (St. Louis, MO). Stock YOYO-1 and 20-nm carboxylate-modified FluoSpheres were purchased from Molecular Probes (Eugene, OR). EcoRI was purchased from Promega (Madison, WI). Microscope cover slips (0.13 mm thick) were purchased from Fisher Scientific (Pitts-

burgh, PA). Ultrapure water was prepared by a Milli-Q purification system (Millipore, Bedford, MA).

## RESULTS AND DISCUSSION

**Design of Nanoparticle Probes.** We have used the restriction enzyme EcoRI and  $\lambda$ -DNA as a model system to study the DNA-binding properties of bioconjugated nanoparticles (Figure 2, A to D). EcoRI (MW = 31 kD) is a site-specific endonuclease that functions as a dimer and recognizes the hexanucleotide sequence GAATTC through 12 hydrogen bonds in the major groove of a duplex DNA molecule.<sup>22,23</sup> Lambda bacteriophage DNA contains five EcoRI restriction sites, all on one half of the molecule. In Figure 2B are shown a number of possible situations in which one or more sites are occupied by EcoRI-conjugated nanoparticles. A further feature is that EcoRI contains a total of 22 lysine residues, one or more of which can be linked to carboxylate groups on the particle surface. Woodhead and Malcolm<sup>24</sup> have found that selected modification of lysine residues yields EcoRI with enzyme activity.

Schwartz and co-workers<sup>25</sup> have also used restriction enzymes to recognize and cleave single stretched DNA molecules at sequence-specific sites. Their work shows that these enzymes can recognize specific sequences even when the target DNA is immobilized and intercalated. However, the bioconjugated nanoparticles are larger than free enzymes and may have difficulties in binding to specific sequences on immobilized DNA molecules. To avoid this problem, we incubated the nanoparticles and DNA in solution, prior to DNA stretching and immobilization. In the presence of magnesium ions (Mg<sup>2+</sup>), we found that this process resulted in rapid cleavage of  $\lambda$ -DNA into fragments. Conventional gel electrophoresis showed that the conjugated enzyme molecules were still active in DNA cleavage. In the absence of magnesium ions, the nanoparticle probes efficiently bound to DNA, but enzymatic cleavage did not take place. Thus, when single DNA molecules are stretched into linear lines, fluorescence imaging can be used to reveal the locations of bound nanoparticles, as discussed below.

**Manipulation of Single DNA Molecules:** T4 DNA and  $\lambda$ -DNA molecules were stretched into linear forms by using hydrodynamic frictional forces on the order of 4–5 piconewtons (pN), as reported in the literature.<sup>21</sup> The stretched DNA was immobilized through strong electrostatic interactions between the negatively charged phosphate groups on the DNA and the surface positive charges. Finding the appropriate polylysine surface charge density was the key to effective DNA stretching and immobilization. On a highly concentrated polylysine-modified surface, DNA molecules tended to condense and fix too strongly to the surface; if the charge density was too low, the stretched DNA molecules moved freely or did not bind to the surface. Spreading 10  $\mu$ L of a 5.5  $\mu$ g/mL polylysine solution between two cover slips yielded

(22) (a) Greene, P. J.; Gupta, M.; Boyer, H. W.; Brown, W. E.; Rosenberg, J. M. *J. Biol. Chem.* **1981**, *256*, 2143–2153. (b) McClarin, J. A.; Frederick, C. A.; Wang, B. C.; Greene, P.; Byer, H. W.; Grable, J.; Rosenberg, J. M. *Science (Washington, D.C.)* **1986**, *234*, 1526–1541.

(23) Newman, A. K.; Rubin, R. A.; Kim, S.-H.; Modrich, P. *J. Biol. Chem.* **1981**, *256*, 2131–2139.

(24) Woodhead, J. L.; Malcolm, A. D. B. *Nucleic Acids Res.* **1980**, *8*, 389–402.

(25) (a) Wang, Y. K.; Huff, E. J.; Schwartz, D. C. *Proc. Natl. Acad. Sci. U.S.A.* **1995**, *92*, 165–169. (b) Meng, X.; Benson, K.; Chada, K.; Schwartz, D. C. *Nature (London)* **1995**, *376*, 432–438.



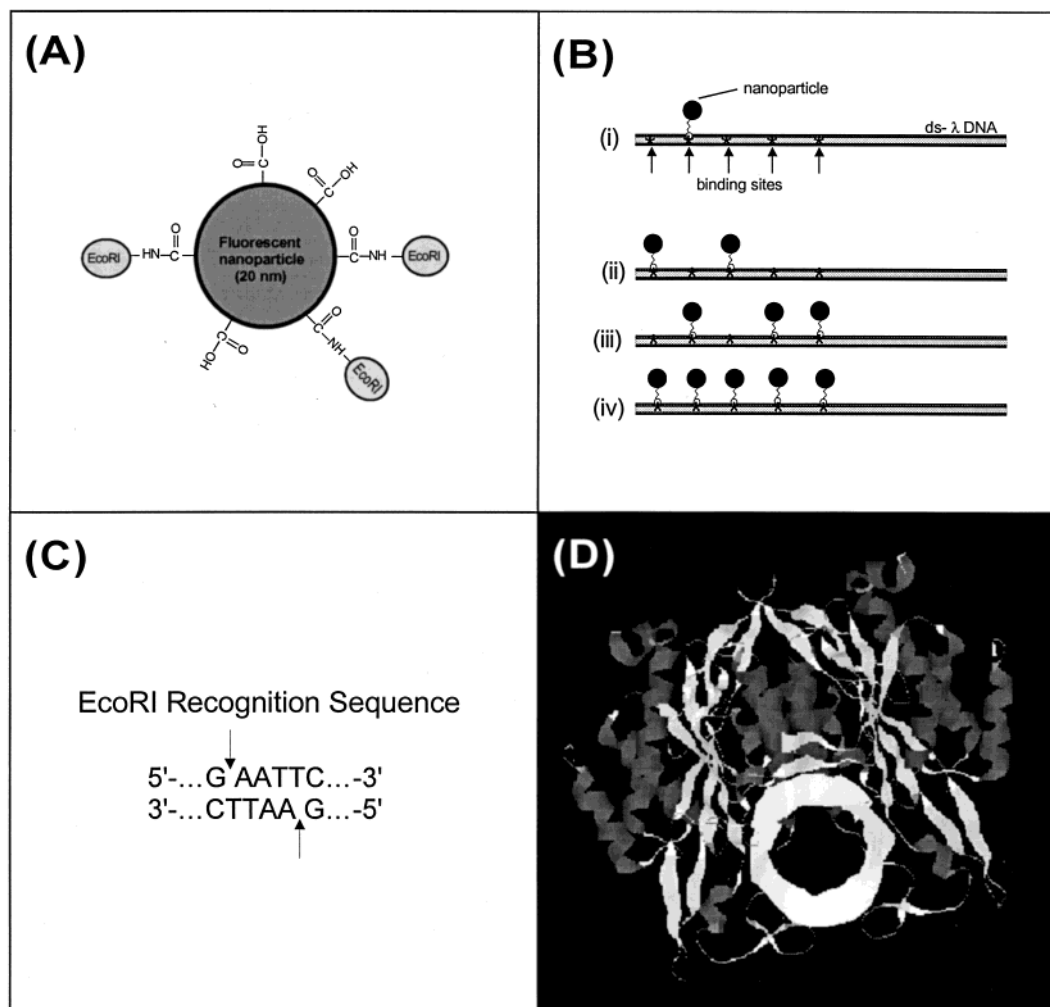


Figure 2. Schematic illustration of (A) EcoRI molecules covalently conjugated to a 20-nm fluorescent nanoparticle, (B) single  $\lambda$ -DNA molecules with 1–5 nanoparticles bound at specific sites, (C) DNA sequence recognized by EcoRI (the cutting sites are indicated by arrows), and (D) EcoRI dimer bound to double-stranded DNA (white circle).

the appropriate surface charge density for consistent stretching. Figure 3A shows a representative fluorescence image of three linearly stretched T4 DNA molecules. Previous studies have shown that DNA molecules can be stretched up to 1.7 times their contour length with forces as great as 80 pN.<sup>3,4</sup> Forces as large as 500–1000 pN are required to break double-helix DNA. Thus, the hydrodynamic forces in our study were sufficient for stretching, but were not strong enough to cause fragmentation. However, double-stranded DNA breaks were occasionally observed as visible gaps on the stretched DNA. As reported by Lyon et al.,<sup>21</sup> these breaks are caused by reactive species such as singlet oxygen and hydroxyl radicals that are generated by optical excitation of the intercalation dye. Such reactive molecules can chemically cleave double-stranded DNA.

A number of research groups have reported success in stretching and fixing large DNA molecules.<sup>25–27</sup> It is believed that the unique laminar-flow profile allows DNA molecules to be

electrostatically attached to the surface, where the liquid flow velocity is zero. The two ends of a DNA molecule are free to move and should have a higher probability of contacting the surface. Such an attachment leads to a rapid stretching and fixing process, similar to “zippering.” The middle sections are less likely to attach to the surface because of restraints by the surrounding DNA segments. The latter type of attachment occurs only occasionally, leading to DNA molecules stretched and fixed in the form of a curve.<sup>28</sup> Recent research using fluorescence video microscopy has examined the stretching process in real time (30 frames per second), and the result supports the mechanism discussed above.<sup>21</sup>

**Nonspecific Binding of Nanoparticles to DNA.** To investigate whether the nonconjugated nanoparticles would randomly bind to DNA, coliphage T4 DNA was incubated with the original carboxylate nanoparticles for 1 h in a Tris/EDTA buffer at 37 °C. Figure 3B shows a multicolor fluorescence image of a stretched T4 DNA molecule (blue) and a number of scattered nanoparticles (yellow). The result indicates that there is little or no interaction between the original nanoparticles and the DNA molecules. This

(26) Bensimon, A.; Simon, A.; Chiffasudel, A.; Croquette, V.; Heslot, F.; Bensimon, D. *Science (Washington, D.C.)* **1994**, *265*, 2096–2098.

(27) (a) Yokota, H.; Johnson, F.; Lu, H.; Robinson, R. M.; Belu, A. M.; Garrison, M. D.; Ratner, B. D.; Trask, B. J.; Miller, D. L. *Nucleic Acids Res.* **1997**, *25*, 1064–1070. (b) Yokota, H.; Nickerson, D. A.; Trask, B. J.; Engh, G.; Hirst, M.; Sadowski, I.; Aebersold, R. *Anal. Biochem.* **1998**, *264*, 158–164.

(28) Allemand, J. F.; Bensimon, D.; Jullien, L.; Bensimon, A.; Croquette, V. *Biophys. J.* **1997**, *73*, 2074–2070.

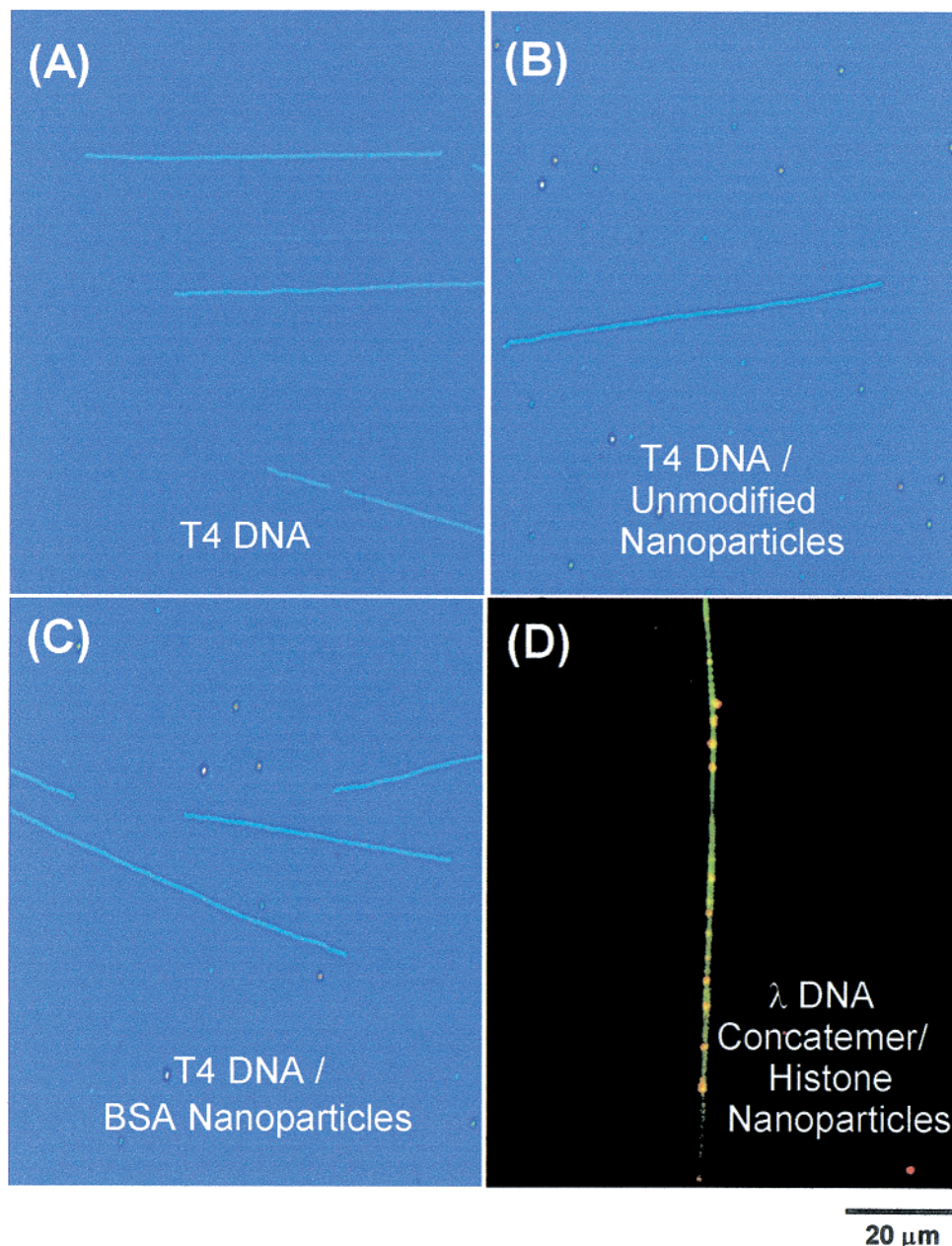


Figure 3. Nonspecific binding of fluorescent nanoparticles to single DNA molecules. (A) Stretched T4 DNA (blue lines) visualized by fluorescence intercalation (YOYO-1). (B) T4 DNA (blue) incubated with the original carboxylate nanoparticles (yellow) and stretched on a glass surface (no binding). (C) T4 DNA (blue) incubated with BSA conjugated nanoparticles (yellow) and stretched on glass (no binding). (D)  $\lambda$ -concatemer DNA (green) incubated with histone-conjugated nanoparticles (yellow) and stretched on glass (random binding). Note that (D) is a true-color image.

finding can be explained by the strong electrostatic repulsion between the negative carboxylate groups on the particle surface and the negative charges on the DNA phosphate backbone. In another control study, T4 and  $\lambda$ -DNA molecules were incubated with BSA conjugated nanoparticles. Again, multicolor fluorescence imaging shows that there is little interaction between the BSA conjugated nanoparticles and the stretched DNA (Figure 3C).

In a further test, we conjugated the nanoparticles to a histone protein. This protein contains a large number of lysine and arginine amino acids and binds to DNA nonspecifically by strong electrostatic attraction.<sup>29</sup> Figure 3D shows a color photograph obtained with a 35-mm camera attached to the front port of the microscope. The stretched DNA molecule emits green fluorescence (dye intercalation), while the histone-conjugated nanopar-

ticles emit yellow-orange fluorescence. As expected, the histone-conjugated nanoparticles bind to the stretched DNA in a random fashion.

**Specific Binding of Nanoparticles to DNA.** In contrast to random histone binding, site-specific binding was observed when EcoRI conjugated particles were incubated with  $\lambda$ -DNA. In Figure 4 are shown representative CCD images (in pseudocolor for better contrast) of  $\lambda$ -DNA molecules with single-site occupancy; that is, only one site on each DNA is occupied by binding to an EcoRI conjugated nanoparticle. The position of each bound particle is determined by a normalization procedure, in which the length of

(29) (a) Van Holde, K. E. *Chromatin*; Springer-Verlag Press: New York, 1988.  
(b) Revzin, A. *The Biology of Nonspecific DNA-Protein Interactions*; CRC Press: Boca Raton, Florida, 1990.



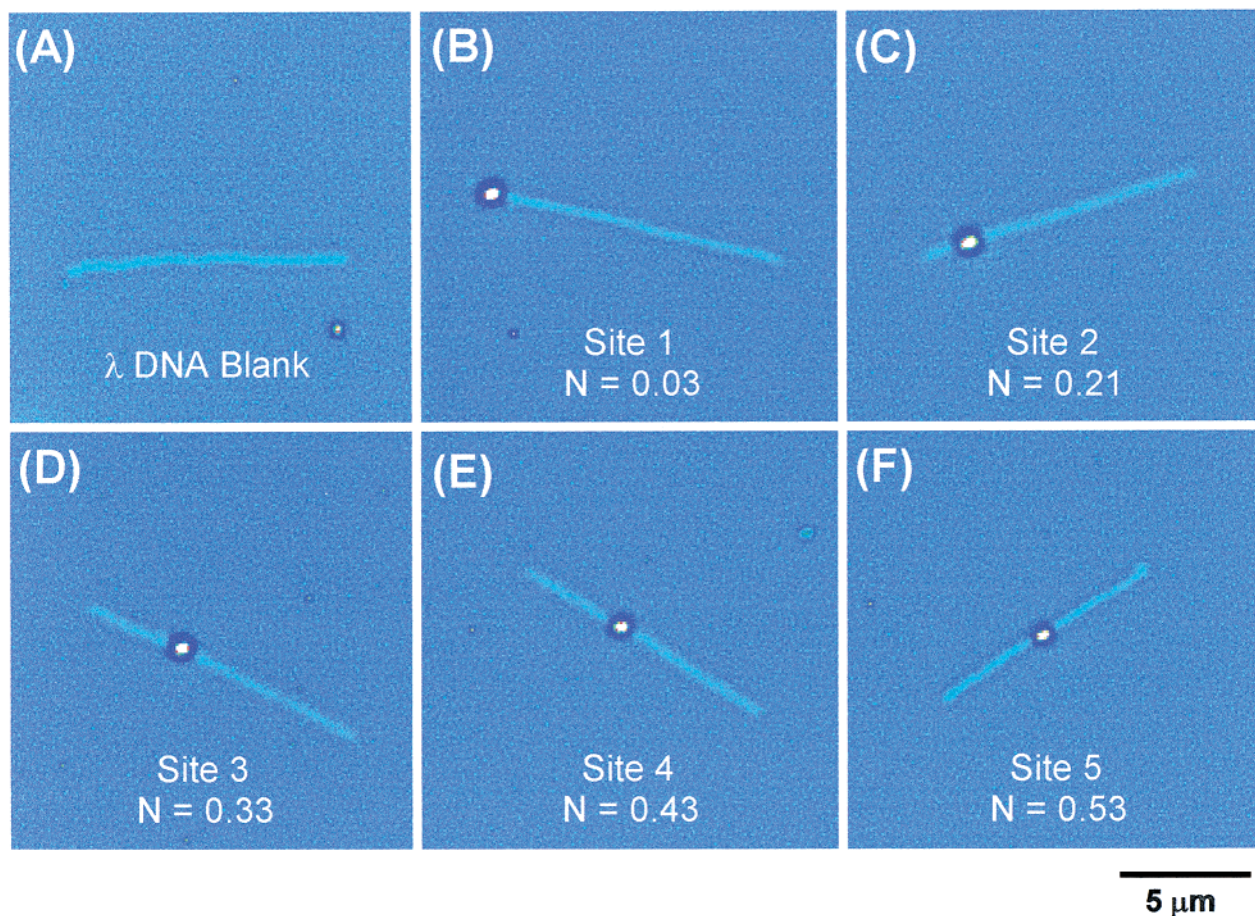


Figure 4. Specific binding of EcoRI conjugated nanoparticles to single  $\lambda$ -DNA molecules. Image (A) is a stretched DNA without binding particles. Images (B) to (F) show single nanoparticles bound to sites 1–5.  $N$  denotes the normalized experimental position for the bound particles.

stretched DNA at the probe is divided by the total DNA length. Unlike the absolute positions of the bound probes, the normalized values remain constant even when DNA molecules are not stretched to the same length (as long as the stretching is uniform along the DNA). Figure 5 shows pseudocolor images of  $\lambda$ -DNA molecules with as many as three bound EcoRI conjugated nanoparticles. This result demonstrates that multiple sequences can be probed simultaneously along the same DNA molecule. However, DNA molecules with five bound particles (i.e., all five sites bound to nanoparticles) were rarely observed. The reason is most likely statistical and not fundamental, because the probability of finding five particles on a single DNA molecule is extremely small under our experimental conditions.

To investigate whether the fluorescence signals arise from single particles or aggregates, we quantitatively measured the signal intensities in a line plot (Figure 6). The peaks correspond to positions where the nanoparticles are bound to DNA. Statistical data on a large number of bound nanoparticles reveal that all the signals have similar intensities. These results provide strong evidence that only a single particle is bound at each specific site. On the other hand, if each site contained an aggregate, the signal intensities would be expected to vary from site to site.

Table 1 summarizes the normalized experimental and theoretical positions for the EcoRI sites on  $\lambda$ -DNA. A strong correlation is found between the theoretical and experimental values for restriction sites 2–5. However, a large deviation is found for the

first restriction site. In fact, the first EcoRI site is close to one end of the DNA which often forms a coil and is difficult to stretch. This uncertainty leads to larger errors in distance measurement. Apart from this site, the observed excellent correlation provides strong evidence for sequence-specific binding on single  $\lambda$ -DNA molecules.

EcoRI is known to bind randomly to a DNA molecule and then slide along the molecule until it reaches a specific sequence.<sup>30–33</sup> Thus, prolonged incubation of DNA with low protein concentrations results in migration of nonspecifically bound molecules to the specific sites. The nonspecifically bound proteins have faster dissociation kinetics and can be washed off using pure buffer. For example, the nonspecifically bound EcoRI has a lifetime ( $\tau_{1/2}$  of dissociation) of 0.1–10 s (depending on electrolyte concentration and DNA length), while the specific complex has a lifetime of

- (30) (a) Terry, B. J.; Jack, W. E.; Rubin, R. A.; Modrich, P. *J. Biol. Chem.* **1983**, *258*, 9820–9825. (b) Terry, B. J.; Jack, W. E.; Modrich, P. *J. Biol. Chem.* **1985**, *260*, 13130–13137. (c) Jack, W. E.; Terry, B. J.; Modrich, P. *Proc. Natl. Acad. Sci. U.S.A.* **1982**, *79*, 4010–4014.
- (31) (a) Halford, S. E. *Trends Biochem. Sci.* **1983**, *12*, 455–460. (b) Rosenberg, J. M.; McClarin, J. A.; Frederick, C. A.; Wang, B.-C.; Grable, J.; Boyer, H. W.; Greene, P. *Trends Biochem. Sci.* **1987**, *10*, 395–398.
- (32) Berg, O. G.; Winter, R. B.; von Hippel, P. H. *Biochemistry* **1981**, *20*, 6929–6948. (b) Winter, R. B.; von Hippel, P. H. *Biochemistry* **1981**, *20*, 6948–6960.
- (33) (a) Ehbrecht, H.-J.; Pingoud, A.; Urbanke, C.; Maass, G.; Gualerz, C. *J. Biol. Chem.* **1985**, *260*, 6160–6166. (b) Langowski, L.; Alves, J.; Pingoud, A.; Maass, G. *Nucleic Acids Res.* **1983**, *11*, 501–513.



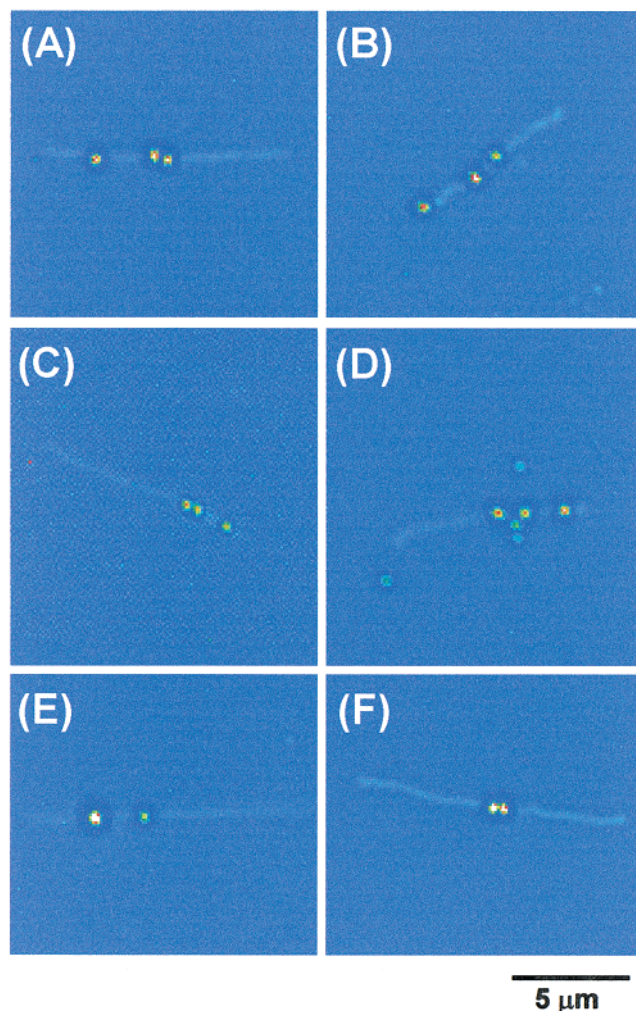


Figure 5. Specific binding of multiple nanoparticles on single  $\lambda$ -DNA molecules. The experimental conditions were similar to those in Figure 4, except that higher nanoparticle concentrations and longer incubation times were used.

about 1 h.<sup>30</sup> These measures can reduce nonspecific binding, but cannot guarantee that all fluorescence signals arise from specifically bound molecules. To address this problem, we examined a large number of stretched DNA molecules and looked for *statistically significant sites*. The basic idea is that specific binding produces a specific pattern on the stretched DNA, while nonspecific binding occurs at random sites. Recent research by Allison et al.<sup>34</sup> indicates that nonspecific binding can be reduced to a very low level, thus allowing direct atomic force imaging of single EcoRI molecules specifically bound to plasmid DNA. We note that statistical measurements are necessary only for the purpose of evaluating the occurrences of specific vs nonspecific binding. Under optimized binding conditions, there is no need to average over a large number of stretched DNA molecules.

It should be pointed out that the nanoparticles are much larger in size than single organic fluorophores, which could create problems in terms of binding kinetics and steric hindrance. Also, nanoparticle probes with multiple copies of fluorophores are not

(34) Allison, D. P.; Kerper, P. S.; Doktycz, M. J.; Spain, J. A.; Modrich, P.; Larimer, F. W.; Thundat, T.; Warmack, R. J. *Proc. Natl. Acad. Sci. U.S.A.* **1996**, *93*, 8826–8829.

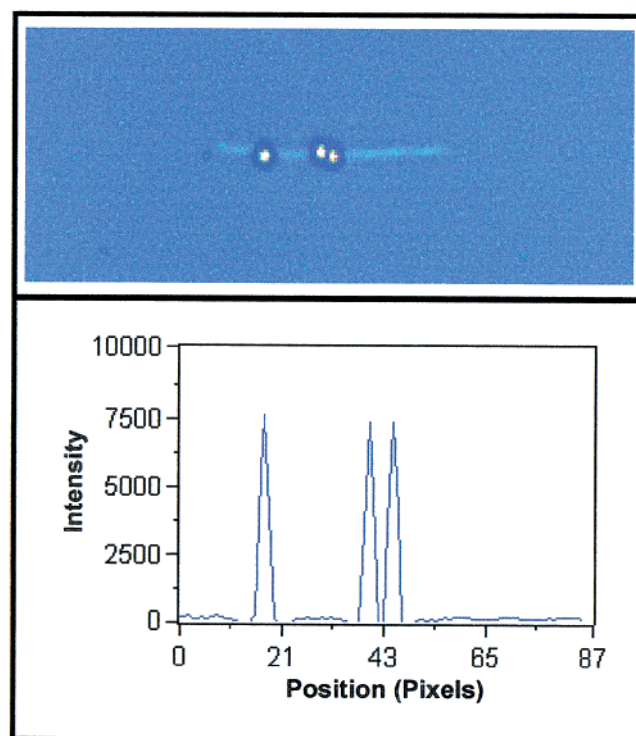


Figure 6. Quantitative analysis of the nanoparticle fluorescence intensities on a single DNA molecule.

Table 1. Comparison of Normalized Experimental and Theoretical Positions for the EcoRI Binding Sites on  $\lambda$ -DNA

	site 1	site 2	site 3	site 4	site 5
literature value ( <i>N</i> )	0.07	0.19	0.35	0.46	0.56
exptl value ( <i>N</i> )	0.03	0.21	0.33	0.43	0.53
std deviation ( <i>s</i> )	( $\pm 0.04$ )	( $\pm 0.02$ )	( $\pm 0.03$ )	( $\pm 0.02$ )	( $\pm 0.01$ )
no. of data points ( <i>n</i> )	32	26	24	20	12

suitable for biomolecular dynamic studies using fluorescence resonance energy transfer (FRET).<sup>35</sup> These problems might be overcome by using luminescent quantum dots in the size range of 2–5 nm. Luminescent quantum dots offer the advantages of size-tunable emission, symmetric spectral shapes, and simultaneous excitation of different quantum dots at a single wavelength.<sup>36</sup> In comparison with rhodamine, research in our group<sup>16</sup> has shown that ZnS-capped CdSe quantum dots are about 20 times brighter and more than 100 times more stable against photobleaching. By linking water-soluble quantum dots to oligonucleotides and proteins, our preliminary data indicate that quantum-dot bioconjugates are especially well suited for prolonged observation and for multiple-color/multi-analyte measurements.

**Applications.** The ability to target specific sequences on single DNA molecules should find applications in rapid gene mapping and in the fundamental study of DNA–protein interactions. For DNA mapping, the achievable accuracies are expected to be about

(35) (a) Ha, T.; Enderle, Th.; Ogletree, D. F.; Chemla, D. S.; Selvin, P. R.; Weiss, S. *Proc. Natl. Acad. Sci. U.S.A.* **1996**, *93*, 6264–6268. (b) Ha, T.; Zhuang, X.; Kim, H. D.; Orr, J. W.; Williamson, J. R.; Chu, S. *Proc. Natl. Acad. Sci. U.S.A.* **1999**, *96*, 9077–9082.

(36) Alivisatos, A. P. *Science (Washington, D.C.)* **1996**, *271*, 933; *J. Phys. Chem.* **1996**, *100*, 13226.



5–10%, as determined by the uniformity of DNA stretching and the optical diffraction limit. This method only requires the binding of nanoparticle probes at specific sites, while the optical mapping method developed by Schwartz and co-workers requires enzymatic cleavage at specific sequences and the generation of visible gaps.<sup>25</sup> Direct optical mapping could improve throughputs, but its accuracy and reproducibility are not much better than those of current DNA mapping and sizing techniques such as pulsed-field gel electrophoresis,<sup>37</sup> single-molecule flow cytometry,<sup>38</sup> and single-fiber fluorescence in-situ hybridization (FISH).<sup>39</sup> On the other hand, the improved photostability and brightness of bioconjugated nanoparticles will provide significant advantages in the real-time observation and dynamic studies of proteins and enzymes bound to single DNA molecules. In particular, we envision that the nanoparticle probes may be used to examine (a) how a protein molecule finds its specific site among a sea of nonspecific sites<sup>30–33</sup> and (b) whether an RNA polymerase moves in a continuous or

an inchworm fashion during active transcription.<sup>40,41</sup> Both questions have been the subject of much interest and debate in biochemistry. Clever single-molecule investigations in the future could yield definite answers to these and other related questions.

## CONCLUSIONS

We have conjugated DNA binding proteins to fluorescent nanoparticles to target specific sequences on stretched single DNA molecules. The attached proteins maintain specific DNA binding and cleavage activities, while the nanoparticles emit intense and stable fluorescent light. The use of fluorescent nanoparticle bioconjugates solves some of the problems associated with single fluorophores such as rapid photobleaching and blinking. The results demonstrate the feasibility of mapping sequence-specific sites on simple genomic DNA molecules. The ability to target specific sequences on single DNA molecules should allow real-time observation of DNA–protein binding and enzymatic dynamics, such as DNA replication and transcription.

## ACKNOWLEDGMENT

This work was supported by the National Science Foundation (CHE-9610254) and the Beckman Foundation Young Investigator Program.

Received for review November 18, 1999. Accepted February 17, 2000.

AC9913311

- 
- (37) Schwartz, D. C.; Cantor, C. R. *Cell* **1984**, *37*, 67.  
 (38) (a) Van Orden, A.; Cai, H.; Goodwin, P. M.; Keller, R. A. *Anal. Chem.* **1999**, *71*, 2108. (b) Van Orden, A.; Keller, R. A.; Ambrose, W. P. *Anal. Chem.* **2000**, *72*, 37.  
 (39) (a) Weier, H.-U. G.; Wang, M.; Mullikin, J. C.; Cheng, J.-F.; Greulich, K.; Bensimon, A.; Gray, J. *Hum. Mol. Genet.* **1995**, *4*, 1903. (b) Michalet, X.; Ekong, R.; Fougereux, F.; Rousseaux, S.; Schurra, C.; Hornigold, N.; Van Slegtenhorst, M.; Wolfe, J.; Povey, S.; Beckmann, J. S.; Bensimon, A. *Science (Washington, D.C.)* **1997**, *277*, 1518.  
 (40) Wang, D.; Meier, T. I.; Chan, C. L.; Feng, G.; Lee, D. N.; Landick, R. *Cell* **1995**, *81*, 341–350.  
 (41) Nudler, E.; Goldfarb, A.; Kashlev, M. *Science (Washington, D.C.)* **1994**, *265*, 793–796.